Journal of Solid State Chemistry **161,** 319–326 (2001)
doi:10.1006/jssc.2001.9320, available online at http://www.idealibrary.com on IDEAL®

Dependence of Boehmite Thermal Evolution on Its Atom Bond Lengths and Crystallite Size

X. Bokhimi,*,†,[1] J. A. Toledo-Antonio,* M. L. Guzmán-Castillo,* B. Mar-Mar,* F. Hernández-Beltrán,* and J. Navarrete*

*Instituto Mexicano del Petróleo, Eje Central L. Cárdenas 152, A.P. 14-805, 07730 México D.F., Mexico; and †Institute of Physics, The National University of Mexico (UNAM), A.P. 20-364, 01000 México D.F., Mexico

Received March 28, 2001; in revised form July 6, 2001; accepted July 23, 2001

The thermal properties of boehmite with a crystallite size between 1 and 27 nm were analyzed by thermogravimetry and differential thermal analysis, and correlated with its crystallography, crystallite morphology, and the atom bond lengths determined by refining its crystalline structure with the Rietveld method. Boehmite's thermal evolution depended on atom bond lengths: the dehydratation temperature was determined by the interaction between an aluminum atom and the oxygen atom of hydroxyl. After dehydratation, the number of hydroxyls in crystals was larger than expected from stoichiometry, because oxygen atoms on crystal surfaces perpendicular to the (020) plane reacted with hydrogen and hydroxyls in environment. The transition temperature from boehmite into γ-alumina was determined by the hydrogen bond in boehmite. The transformation temperature from transitional aluminas into α-Al_2O_3 also varied with boehmite's crystallite size; however, it was not determined by the amount of hydroxyls in transitional aluminas, but probably by the aluminum–oxygen bonds in boehmite. © 2001 Academic Press

Key Words: **boehmite; water adsorption; atomic bond lengths; transformation temperature; γ-alumina; transitional aluminas; α-alumina.**

INTRODUCTION

Transitional aluminas are widely used as catalysts, catalyst supports, adsorbents, coatings, ceramics, and abrasives (1–4). In general, they are prepared by dehydroxylation of aluminum hydroxides $Al(OH)_3$ (gibbsite and bayerite) or aluminum oxyhydroxides AlOOH (boehmite and diaspore), which determine alumina's final properties. Therefore, the thermal transformation of these hydroxides and oxyhydroxides into transitional aluminas has been studied intensively (5–11). Of them boehmite has been the most studied (13, 14), because it is widely used in industry (12).

When boehmite is annealed, it undergoes a series of polymorphic phase transformations: from boehmite into γ-alumina and then into δ- and θ-alumina, which are known as transitional aluminas, and eventually into α-alumina, the thermodynamically most stable alumina phase (15). The transformation of boehmite into γ-Al_2O_3 is endothermic and occurs after partial dehydroxylation between 300 and 550°C, while the transformation of transitional aluminas into α-Al_2O_3 is exothermic and requires complete dehydroxylation, which occurs between 800 and 1300°C. The transformations of γ- into δ- and θ-alumina proceeds pseudomorphically (11), requiring only small amounts of energy that are hardly detected in DTA experiments. Transformation temperatures strongly depend on boehmite "crystallinity"—boehmite with low "crystallinity" traditionally has been named pseudoboehmite, which has been assumed to have water molecules in its crystalline structure (16, 17).

It was demonstrated, however, that boehmite and pseudoboehmite are the same crystalline phases but with different crystallite size (18, 19), and that pseudoboehmite does not have intercalated water in its structure as has been claimed by many authors (16, 17, 20, 21). Because boehmite's atomic bond lengths and bond angles depend on its crystallite size (19), it is interesting to study how they affect the properties of γ- and α-aluminas derived from boehmite, which are known to depend on synthesis conditions: pH (22, 23), digesting (24) and aging time (25), and synthesis routes (26–28). It is worth mentioning that γ-alumina crystallite size depends on the crystallite size of its precursor boehmite.

In this paper, we report how boehmite's crystallite size and atomic bond lengths correlate with water desorption, transformation temperature of boehmite into γ-alumina, and the transformation temperature of transitional aluminas into α-alumina. Transition temperatures and weight loss were determined via thermogravimetry (TG) and differential thermal analysis (DTA), and the evolution of hydroxyls was followed with infrared spectroscopy.

[1] To whom correspondence should be addressed. E-mail: bokhimi@fenix.ifisicacu.unam.mx.

0022-4596/01 $35.00

Boehmite's crystallography and crystal morphology were analyzed with X-ray powder diffraction and the crystalline structure was refined via the Rietveld method.

EXPERIMENTAL

Sample Preparation

Boehmite seeds were annealed under hydrothermal conditions at specific temperatures to get different crystallite sizes. Seeds were precipitated at room temperature by simultaneously dropping two aqueous solutions into 50 mL of distilled water at pH 8. The first solution (300 mL, 0.3 M Al^{3+}) was prepared by dissolving $AlCl_3 \cdot 6H_2O$ (J. T. Baker) in distilled water; the second one (100 mL) was prepared by dissolving NH_4OH (J. T. Baker, 50 vol%) in distilled water. The suspension (450 mL) with the precipitated boehmite seeds was placed in the 600-mL autoclave vessel and heated at a fixed temperature between 23 and 240°C for 18 h under autogenous pressure, stirring continuously. Thereafter, the suspension was filtered and washed thoroughly several times with distilled water until it was chlorine free, according to silver nitrate test; the washed suspension was eventually dried overnight at 110°C in air.

Characterization

X-ray diffraction. X-ray diffraction patterns of the samples packed in a glass holder were recorded at room temperature with Cu$K\alpha$ radiation in a Bruker Advance D-8 diffractometer that had Θ–Θ configuration and a graphite secondary beam monochromator. The diffraction intensity was measured in the 2θ range between 10 and 127°, with a 2θ step of 0.02° for 8 s per point. Crystalline structures were refined with the Rietveld technique by using DBWS-9411 (29) and FULLPROF-V3.5d (30) codes; peak profiles modeled with pseudo-Voigt functions (31) contained average crystallite size as one of its characteristic parameters (32). Standard deviations, which show the last figure variation of a number, are given in parentheses; when they correspond to refined parameters, their values are not estimates of the probable error in the analysis as a whole, but only of the minimum possible probable errors based on their normal distribution (33).

Thermoanalysis. Weight loss and temperatures associated with phase transformations were determined by thermogravimetry and differential thermal analysis with a Perkin-Elmer TG-7 and a Perkin-Elmer 1700 apparatus, respectively. To enhance the peaks associated with transformations, samples were heated in a static atmosphere from room temperature to 1400°C at 10°C/min. DTA was carried out using platinum crucibles and α-alumina as reference.

Infrared spectroscopy. FTIR spectra were measured on a Nicolet Protege 460, which had a resolution of 4 cm^{-1}. The sample powder was mixed with KBr (2%) and pressured into thin disks to be measured in a Pyrex cell that had CsI windows.

RESULTS AND DISCUSSION

Crystallite Size

Boehmite was the only phase observed in all fresh samples (Fig. 1). The crystalline structure was refined by modeling it with an orthorhombic unit cell with the symmetry described by space group *Cmcm*; more details of the refinement are given elsewhere (19). Diffraction peak widths depended on Miller indices; the widest one corresponded to the (020) reflection, indicating that the crystallite's shortest dimension was parallel to the [020] direction, and corroborating the platelike form of boehmite crystallites (34). This dimension, represented as $d_{(020)}$, corresponds to crystal thickness and depends on the hydrothermal heating temperature (Table 1).

Boehmite's average crystallite thickness varied from nearly a unit cell, 1.13(1) nm, to 26.3(5) nm for the samples crystallized at 23 and 240°C, respectively. Along the crystallite plate, the average dimension, which is represented as $d_{(002)}$ in Table 1, grew from 3.21(8) to 49(1) nm for 23 and 240°C, respectively; the smallest dimension along the plate,

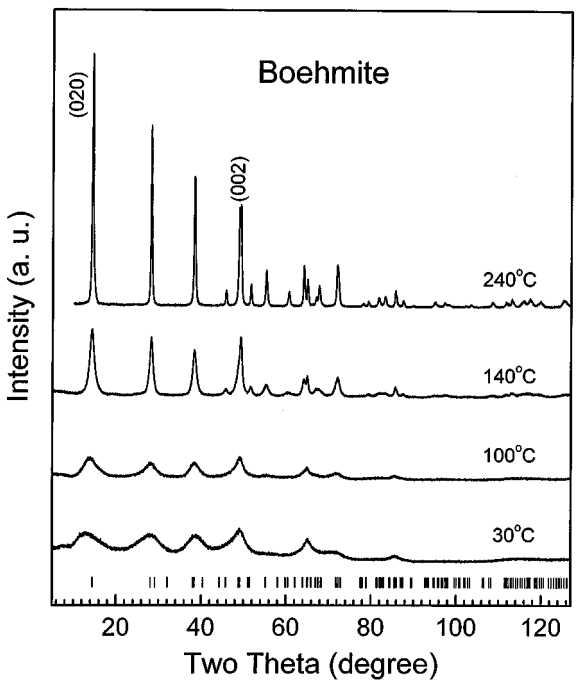

FIG. 1. X-ray diffraction patterns of the samples annealed under hydrothermal conditions at temperatures between 30 and 240°C. Tic marks correspond to boehmite. Because they are specially mentioned in tables, (020) and (002) reflections are also indicated.

TABLE 1
Boehmite's Crystallite Size and d_{Al-OH} Bond Length as a Function of Synthesis Temperature

T (°C)	$d_{(020)}$ (nm)	$d_{(002)}$ (nm)	d_{Al-OH} (nm)
23	1.13(1)	3.21(8)	0.1810(1)
30	1.56(2)	3.53(8)	0.1825(1)
50	2.04(4)	4.0(1)	0.1805(1)
100	2.42(4)	5.4(1)	0.1823(1)
140	6.90(8)	16.6(4)	0.1892(1)
180	14.2(2)	43(2)	0.1901(1)
240	26.3(5)	49(1)	0.1904(1)

3.21(8) nm, was nearly 10 times the unit cell lattice parameter (a and c) along the plate, indicating that boehmite crystals grew with preference along plates. Because crystallite thickness occurs along one crystallographic axis (b axis), it is a well-defined crystal dimension that can be used as representative of crystallite size; therefore, in the following discussion, it will be used to identify boehmite's crystallite dimensions (19).

Thermal Analysis

Boehmite samples had a significant weight loss below 200°C (Fig. 2) produced by water desorption (Fig. 3); the amount of desorbed water molecules relative to the number of AlOOH units in crystal versus crystallite size decreased as size increased, following a hyperbola (Table 2 and Fig. 4). Because the dependence of the surface-to-bulk ratio on the crystallite thickness followed the same relationship ($1/d_{(020)}$), these water molecules should be uniformly distributed on boehmite's crystallite surface.

The weight loss observed between 200 and 550°C (Fig. 2) was produced by the partial dehydroxylation occurring when boehmite transformed into γ-alumina (Fig. 3); this transformation temperature depended on the crystallite size (Table 3 and Figs. 2 and 5). The structure observed in the absorption band located around 3500 cm^{-1}, which was produced by the stretching vibrations of hydroxyls, indicated that hydroxyls were in more than one local environment. The weight loss between 550 and 1300°C was associated with the further elimination of the residual hydroxyls in the crystalline structure of the transitional aluminas (35, 36). The concentration of these hydroxyls was large, and should play a key role in compensating the cation vacancies in the spinel structure characteristic of transitional aluminas (37).

The total weight loss produced only by hydroxyls (after eliminating adsorbed water) was quantified (Fig. 6) by using the following stoichiometric equation for boehmite transformation:

$$2\gamma\text{-AlOOH} \rightarrow H_2O + Al_2O_3.$$

Ideally, this equation gives rise to a H_2O/Al_2O_3 molar ratio of 1.0; but, in the present study, this ratio strongly depended on boehmite's crystallite size: it decreased as the crystallite size increased, and was approximately 1.0 only for large crystallites. This excess of hydroxyls has been explained by assuming that boehmite's crystalline structure contains water (16, 17), especially in the so-named "pseudoboehmite" (16, 20). This explanation, however,

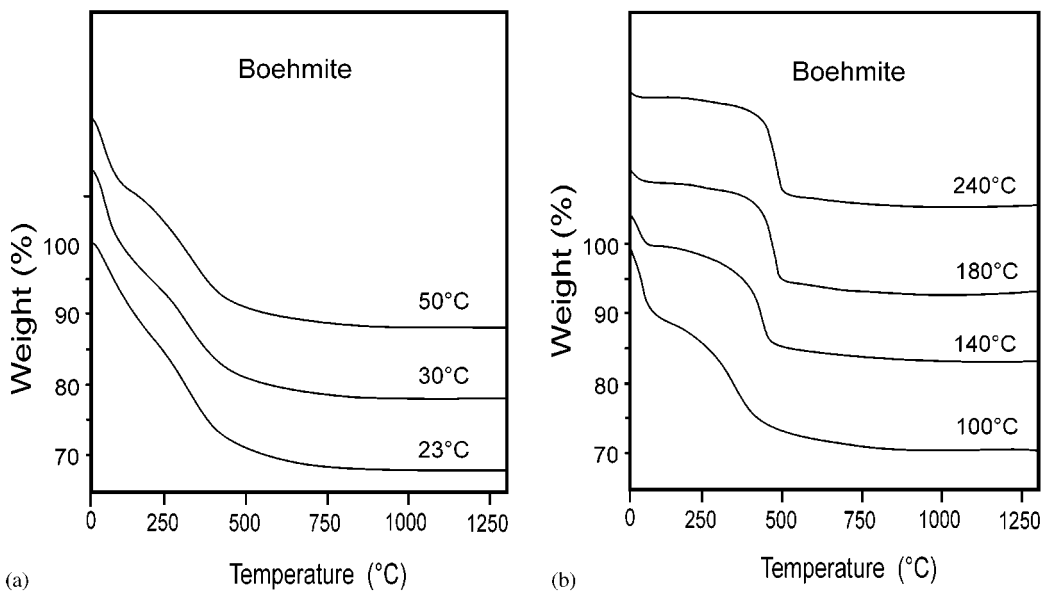

FIG. 2. TG curves of boehmite samples: (a) prepared between 23 and 50°C; (b) prepared between 100 and 240°C.

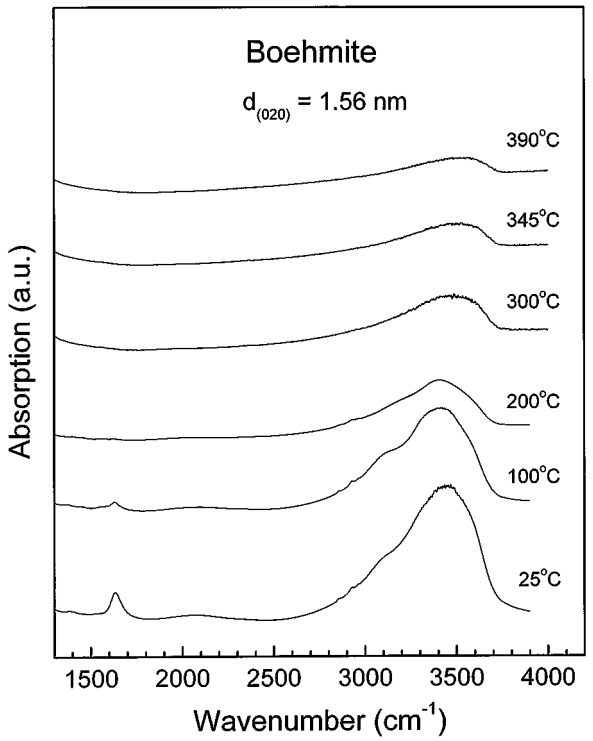

FIG. 3. FTIR spectra of the boehmite sample synthesized at 30°C, $d_{(020)} = 1.56(2)$ nm, after it was annealed *in situ* between room temperature and 390°C in air.

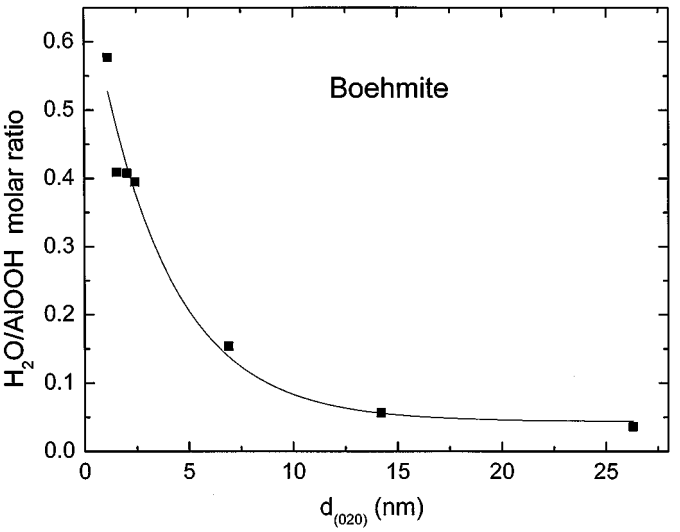

FIG. 4. Amount, quantified via the ratio H_2O/AlOOH, of adsorbed water on boehmite. Points correspond to experimental data; the continuous line is only a visual aid.

should be discarded, because a detailed study on the crystallography of boehmite with different crystallite sizes (19) showed that water molecules cannot be hosted in its crystalline structure (18, 19).

In the present analysis, we are proposing an alternative interpretation for this observed weight loss: boehmite crystallites are made of double layers of octahedra with an aluminum atom near their center and two hydroxyls and four oxygen atoms in their vertices (Fig. 7) (19). The octahedra in the double layers interact strongly with each other, but the interaction between double layers is weak, because it is produced via hydrogen bonds (Fig. 7). This weak interaction causes the crystal surface to end in the interface between two double layers, producing surfaces full of hydroxyls (those in the crystalline structure). On the crystal surfaces parallel to the *b* axis and cutting the double layers, for example the one projected in Fig. 7, the charge of the oxygen atoms should be compensated. This occurs by the reaction of oxygen atoms with the hydrogen or hydroxyls of the environment, causing all of these surfaces to be covered with hydroxyls; the corresponding octahedra then will contain more than the two initial hydroxyls. The local atom distribution around these new surface hydroxyls, however, is different from that of hydroxyls in bulk and on the crystal surfaces parallel to octahedral double layers. When the crystallite size diminished, the number of these new hydroxyls increased, because the area of the surfaces parallel to the *b* axis relative to the total surface increased as the crystallite size decreased, giving rise to larger water/alumina ratios than expected from stoichiometry.

TABLE 2
Water to Boehmite and Alumina Molecular Ratio as a Function of Boehmite's Crystallite Size

$d_{(020)}$ (nm)	H_2O/AlOOH	H_2O/Al_2O_3
1.13(1)	0.577	1.428
1.56(2)	0.409	1.538
2.04(4)	0.408	1.492
2.42(4)	0.395	1.425
6.90(8)	0.154	1.161
14.2(2)	0.057	1.073
26.3(5)	0.036	1.045

TABLE 3
Boehmite Transition Temperature into γ-Alumina and Its Hydrogen Bond Length as a Function of Boehmite's Crystallite Size

$d_{(020)}$	T (°C)	$d_{O-H\cdots O}$ (nm)
1.13(1)	380	0.2765(1)
1.56(2)	403	0.2788(1)
2.04(4)	413	0.2818(1)
2.42(4)	428	0.2803(1)
6.90(8)	471	0.2691(1)
14.2(2)	508	0.2685(1)
26.3(5)	528	0.2681(1)

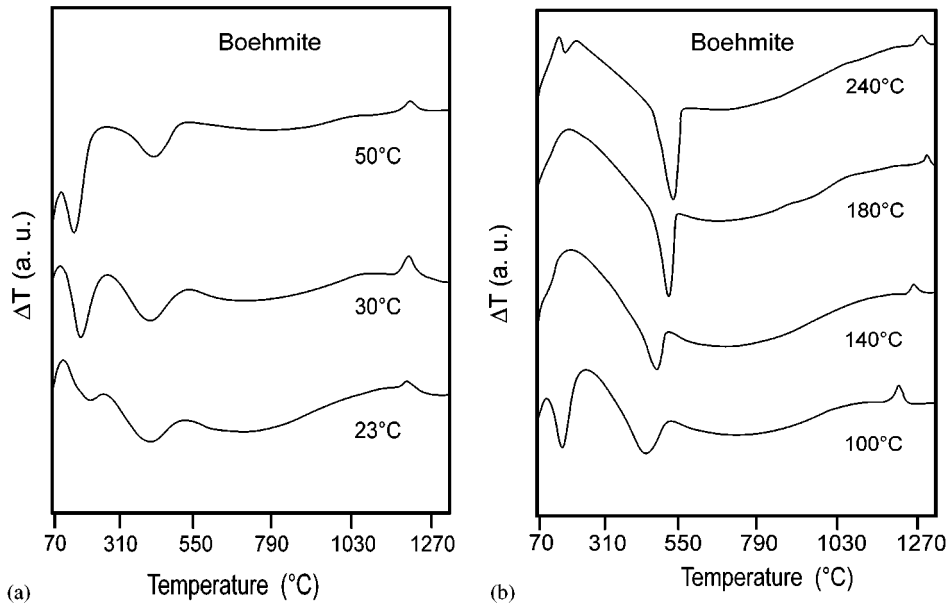

FIG. 5. DTA curves of boehmite samples: (a) prepared between 23 and 50°C; (b) prepared between 100 and 240°C.

When the crystallite size increased, however, the number of these hydroxyls diminished and the water/alumina molar ratio was approximately 1.0.

When boehmite transformed into a transitional alumina, many of the hydroxyls of boehmite remained in the alumina atom distribution, as revealed by the TG and FTIR studies (Figs. 2 and 3). The number of these hydroxyls was estimated by assuming the stoichiometric formula proposed by Soled (37) for the different degrees of boehmite dehydroxylation: $Al_2O_{3-X/2}(OH)_X$; X, varying between 0 and 2, is the number of hydroxyls contained in the transitional aluminas—$X = 2$ corresponds to a completely hydroxylated boehmite, $Al_2O_2(OH)_2$, whereas $X = 0$ corresponds to the totally dehydroxylated α-alumina.

The weight loss observed in transitional aluminas was due to the hydroxyls leaving the crystalline structure

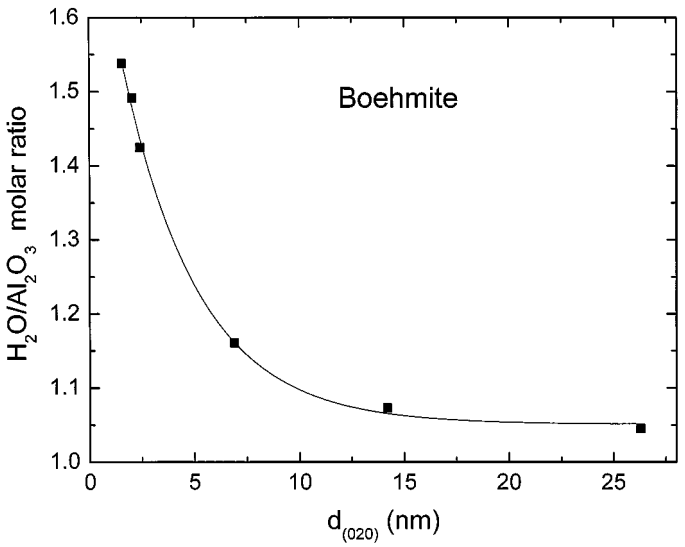

FIG. 6. Amount, quantified via the ratio H_2O/Al_2O_3, of hydroxyls in dehydrated boehmite. Points correspond to experimental data; the continuous line is only a visual aid.

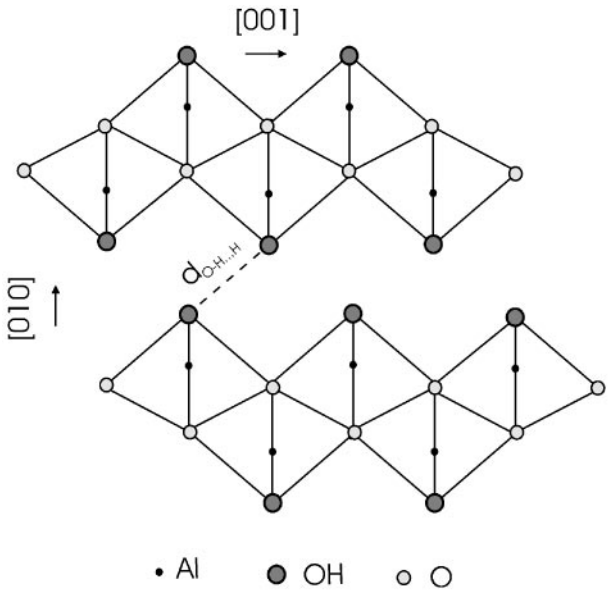

FIG. 7. Boehmite's crystalline structure projected on a plane perpendicular to the [100] direction. Double octahedral layers are held together through hydrogen bonds.

according to the following equation:

$$Al_2O_{3-X/2}(OH)_X \rightarrow Al_2O_3 + X/2H_2O.$$

The number of hydroxyls (X) in the transitional aluminas increased when boehmite's crystallite size increased in the range between 1.13 and 2.5 nm (Fig. 8). But it decreased for sizes larger than 2.5 nm, producing a maximum for the crystallite size of 2.5 nm, which corresponds to the sample synthesized at 100°C. High-resolution electron microscopy of the boehmite samples showed well-defined crystallite morphology when they were synthesized at 100°C and higher temperatures (38); crystallites were plates perpendicular to the [010] direction with lateral surfaces parallel to the $\langle 101 \rangle$ directions and the b axis. The crystallite morphology in the samples synthesized below this temperature was different and not well defined, which could be responsible for the increase of the number of hydroxyls in the alumina derived from boehmite with a crystallite size lower than 2.5 nm. Tsukada *et al.* (17) recently reported that the number of hydroxyls in γ-Al_2O_3 depends linearly on the boehmite crystal size; their analysis, however, was performed for boehmite with crystallite sizes between 4 and 20 nm.

Phase Transitions

When samples were annealed in air, they presented two endothermic peaks below 550°C, and one exothermic peak above 1100°C (Fig. 5). The first endothermic peak, which appeared below 200°C, represents sample dehydratation (Fig. 3). The temperature at which it occurred increased as the crystallite size decreased, indicating that the adsorption energy of water molecules on boehmite surface depended on crystallite size, in accordance with previous reports (17). The crystallography of boehmite with different crystallite sizes (19) shows that the interaction between an aluminum atom and the oxygen atom of hydroxyls increases as the crystallite size decreases (Table 1); consequently, the interaction of the hydroxyls on surface with the molecules of the environment, for example water, is stronger and water desorption will occur at higher temperatures (19). In the industrial applications of boehmite (5, 39), this water desorption as a function of boehmite crystallite size needs to be taken into account because the shrinkage during the dehydration process will depend on it.

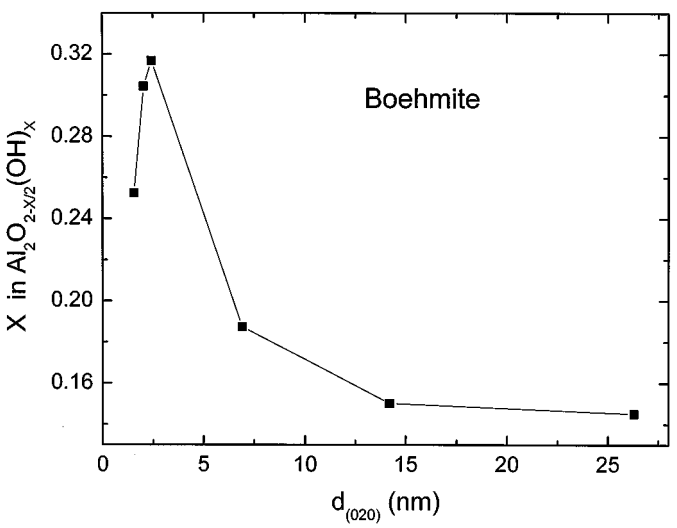

FIG. 8. Number of hydroxyls X in transitional aluminas as a function of crystallite size. Points correspond to experimental data; the continuous line is only a visual aid.

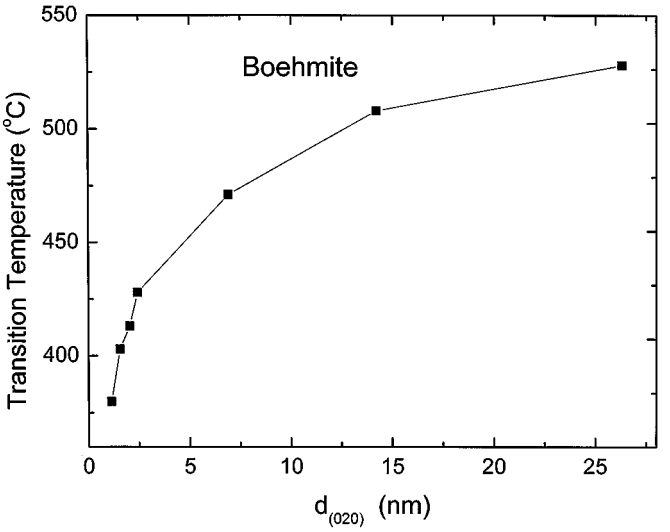

FIG. 9. Transition temperature of boehmite into γ-alumina as a function of boehmite crystallite size. Points correspond to experimental data; the continuous line is only a visual aid.

The second endothermic peak between 300 and 550°C corresponds to the pseudomorphic transition from boehmite into γ-Al_2O_3, which occurs through partial dehydroxylation (Figs. 2 and 3). The associated transition temperature diminished as boehmite crystal size decreased (Table 3 and Fig. 9) and depended on the variation of the hydrogen bonding with the crystallite size.

As described elsewhere (19), the atomic bond lengths and bond angles between atoms in boehmite depend on its crystallite dimensions. Because of its weakness (less than 20 kJ mol^{-1}) (40), the only boehmite bond that can be broken between 300 and 500°C is the hydrogen bond, to which is associated the bond length $d_{O-H\cdots O}$ (Fig. 7). This bond length increases as boehmite's crystal size decreases (Table 3), indicating that the corresponding bond energy decreases. Therefore, these small crystallites require less energy than the large crystals to break this bond, and consequently to destroy boehmite's crystalline structure and to produce its transformation into γ-alumina—the transformation temperature associated with the above

phenomenon ranged from 300 to 550°C, which corresponds to k_BT products between 4.77 and 6.84 kJ mol^{-1} (k_B is the Boltzmann constant and T the absolute temperature in kelvin).

The exothermic peak above 1100°C in DTA profiles (Fig. 5) corresponds to the transformation of transitional aluminas, which are based on the spinel crystalline structure, into the most stable crystalline structure of alumina, the α phase. This transition temperature also depended on boehmite's crystallite size (Fig. 10); the transition occurred at higher temperatures for the boehmite samples with larger crystallite size, in accordance with previous reports (29, 35).

Since the transformation of transitional aluminas into α-Al_2O_3 occurs when their crystallites are completely dehydroxylated, one would expect that the transformation of the more hydroxylated alumina occurred at higher tempeatures (in the present case those with low crystallite size). It was observed, however, that the less hydroxylated alumina (Table 4 and Fig. 8), the one with the largest crystal, transformed into α-Al_2O_3 at the highest temperature, indicating that this phase transition was not determined by the number of hydroxyls in the transitional alumina.

This transition temperature followed a linear relationship when it was compared to the crystallite size of the transition alumina (Fig. 11): for larger crystallites the transition temperature was higher. The analysis of the crystalline structure of the transition alumina was not precise enough to get its atomic bond lengths in order to correlate them with the observed transition temperatures (19). Since these transition temperatures were also related to boehmite's crystallite size (Fig. 9), it is interesting to analyze the dependence of boehmite's bonds as a function of this size in order to find a possible correlation between them and the temperature of the transition to the α phase. This, of course, is partially speculative, but the analysis would motivate us to study in detail some of the transition alumina properties coming from precursors with different crystallite sizes; it is especially important to get their atomic bonds by using appropriate techniques—actually, by using FTIR spectroscopy we are trying to get some information about these bonds to correlate them with boehmite's crystallite size. In another experiment, transitional aluminas, prepared at 788°C in air and coming from boehmite with crystallite sizes of 26.1(1) and 3.32(4) nm (18), were exposed to heavy water (D_2O) steam at 300°C just after they were annealed in air at 300°C to eliminate adsorbed water from the environment. In the sample coming from the boehmite with small crystallites almost all hydroxyls were substituted by OD^- ions, but in the sample coming from the boehmite with the large crystallite the substitution was about one-half. This indicates that the non-interchanged hydroxyls should be in the bulk of the transitional alumina, which is larger in the sample coming from the boehmite with the large crystallite; therefore, these hydroxyls cannot be interchanged.

TABLE 4

Number of Hydroxyls (X) per Formula in Transitional Alumina $Al_2O_{3-X/2}(OH)_X$; γ-Alumina Crystallite Size and the Transformation Temperature into α-Alumina as a Function of Boehmite's Crystallite Size

$d_{(020)}$	X	$d_{\gamma\text{-alumina}}$ (nm)	T (°C)
1.13(1)	0.274	2.65(7)	1190
1.56(2)	0.2526	2.69(7)	1198
2.04(4)	0.3044	3.0(1)	1203
2.42(4)	0.3168	3.3(1)	1206
6.90(8)	0.1874	4.5(1)	1249
14.2(2)	0.1502	6.2(2)	1289
26.3(5)	0.1452	6.6(2)	1290

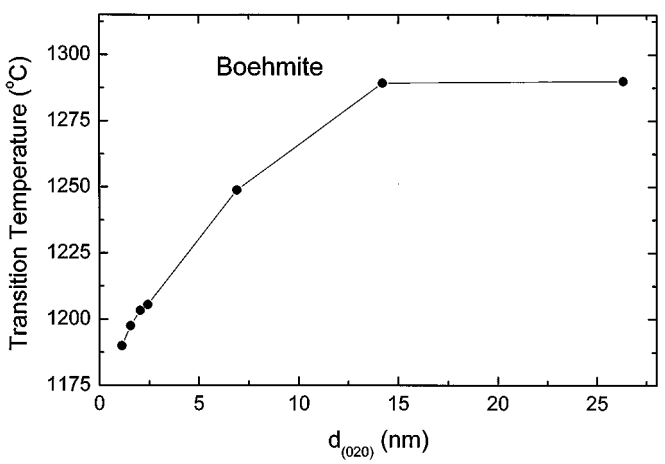

FIG. 10. Transformation temperature of transitional aluminas into α-alumina as a function of boehmite crystallite size. Points correspond to experimental data; the continuous line is only a visual aid.

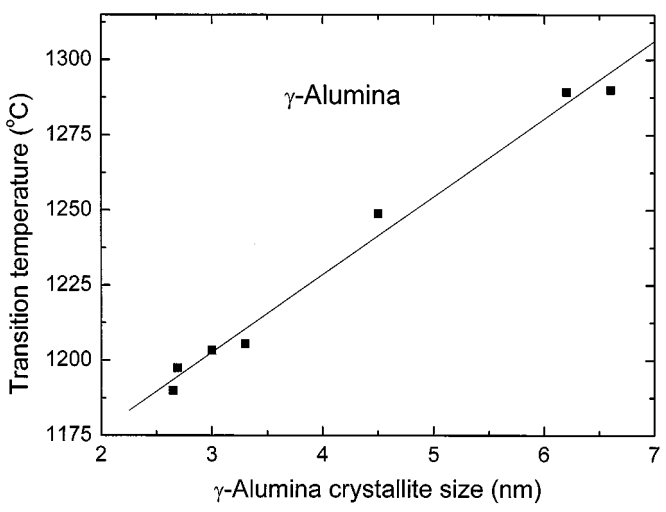

FIG. 11. Transformation temperature of transitional aluminas into α-alumina as a function of transitional alumina crystallite size. Points correspond to experimental data; the continuous line is only a visual aid.

When the bond lengths in the representative octahedron of boehmite are analyzed (19), it is observed that those between oxygen atoms and oxygen and aluminum atoms decrease as boehmite's crystallite size increases [d_2, d_3, and d_7 in Tables 5 and 7 of Ref. (19)], which is equivalent to an increase of the corresponding binding energy. If we assume that this bond length's variation with crystallite size is maintained when boehmite is transformed into a transitional alumina, then transition aluminas with stronger bonds, those with the largest crystallite sizes, would transform into the α phase at higher temperatures, as is observed experimentally. This requirement is equivalent to assuming that during the transformation of boehmite into γ-alumina some boehmite octahedra survive without changing their initial interactions and form part of the alumina crystalline structure; this assumption is supported by the presence of large amounts of hydroxyls even when boehmite is transformed into γ-alumina (Fig. 3) and the fact that some of them are in alumina's bulk. Since the experiments to obtain Fig. 3 were performed *in situ*, the hydroxyls of γ-alumina observed at 390°C came from boehmite and not from the environment.

CONCLUSIONS

Boehmite's thermal evolution depended on atomic bonds and crystallite size. The desorption temperature of adsorbed water on boehmite crystallites surface was determined by the bonds between aluminum atoms and hydroxyls. After water desorption, the amount of hydroxyls leaving the sample when it was further heated was larger than expected from stoichiometry. This was because the oxygen in the octahedral vertices on crystal surfaces perpendicular to the (020) boehmite plane compensated their charge by reacting with hydroxyls and hydrogen in the environment. The transition temperature from boehmite into γ-alumina depended on the hydrogen bond strength between the octahedral double layers that sustain the crystalline structure. The exothermic transformation temperature from transitional aluminas into α-Al_2O_3 varied with boehmite's crystal size: it was larger for the samples with larger crystallites. The temperature was not determined by the amount of hydroxyls in transitional aluminas; it probably is determined by the initial bonding in the precursor boehmite.

ACKNOWLEDGMENTS

We thank Mr. A. Morales and Mr. M. Aguilar for technical assistance. This work was financially supported by projects IMP-D.01024 and IMP-D.01234.

REFERENCES

1. K. Tanabe and W. F. Hölderich, *Appl. Catal. A*: *General* **181,** 399 (1999).
2. P. Grange, *Catal. Rev. Sci. Eng.* **21,** 135 (1980).
3. B. C. Gates, *Chem. Rev.* **95,** 511 (1995).
4. Z. Xu, F. S. Xiao, S. K. Purnell, O. Alexeev, S. Kawai, S. E. Deutsch, and B. C. Gates, *Nature* **372,** 346 (1994).
5. D. L. Trimm and A. Stanislaus, *Appl. Catal.* **21,** 215 (1986).
6. S. Keysar, G. E. Shter, Y. De Hazan, Y. Cohen, and G. S. Grader, *Chem. Mater.* **9,** 2464 (1997).
7. C. Pecharromán, I. Sobrados, J. E. Iglesias, T. González-Carreño, and J. Sanz, *J. Phys. Chem. B* **103,** 6160 (1999).
8. G. V. Rama Rao, S. Venkadesan, and B. Saraswati, *J. Non-Cryst. Solids* **111,** 103 (1989).
9. Ph. Colomban and B. Vendange, *J. Non-Cryst. Solids* **245,** 147 (1992).
10. B. E. Yoldas, *J. Am. Ceram. Soc.* **65,** 387 (1982).
11. B. Balek, E. Klosova, M. Murat, and N. A. Camargo, *Am. Ceram. Bull.* **75,** 73 (1996).
12. M. Chanakya and S. Thinnalur, U.S. Patent 4,595,581, 1986.
13. A. C. Pierre, E. Elaloui, and G. M. Pajonk, *Langmuir* **14,** 66 (1998).
14. S. F. Tikhov, V. B. Fenelonov, V. I. Zaikovskii, Yu. V. Potapova, and V. A. Sadykov, *Microporous Mesoporous Mater.* **33,** 137 (1999).
15. H. L. Wen and F. S. Yen, *J. Cryst. Growth.* **208,** 696 (2000).
16. Z. R. Ismagilov, R. A. Shkrabina, and N. A. Koryabkina, *Catal. Today* **47,** 51 (1999).
17. T. Tsukada, H. Segawa, A. Yasumori, and K. Okada, *J. Mater. Chem.* **9,** 549 (1999).
18. M. L. Guzmán-Castillo, X. Bokhimi, J. A. Toledo-Antonio, J. Salmones-Blásquez, and F. Hernández-Beltran, *J. Phys. Chem.* **105,** 2099 (2001).
19. X. Bokhimi, J. A. Toledo-Antonio, M. L. Guzmán-Castillo, and F. Hernández-Beltrán, *J. Solid State Chem.* **159,** 32 (2001).
20. B. C. Lippens, Doctoral Thesis, Technical University of Delft, Amsterdam, 1961.
21. J. J. Fitzgerald, G. Piedra, S. F. Dec, M. Seger, and G. E. Maciel, *J. Am. Chem. Soc.* **119,** 7832 (1997).
22. J. T. Trawczynski, *Ind. Eng. Chem. Res.* **35**, 241 (1996).
23. K. Hellgardt and D. Chadwick, *Ind. Eng. Chem. Res.* **37**, 405 (1998).
24. G. K. Chuah, S. Jaenicke, and T. H. Xu, *Microporous Mesoporous Mater.* **37,** 345 (2000).
25. Y. Cesteros, P. Salagre, F. Mediana, and J. E. Sueiras, *Chem. Mater.* **11,** 123 (1999).
26. L. Ji, J. Ling, K. L. Tan, and H. C. Zeng, *Chem. Mater.* **12,** 931 (2000).
27. A.Vázquez, T. López, R. Gómez, and X. Bokhimi, *J. Mol. Catal. A* **167,** 91 (2001).
28. A. I. Mamchik, S. V. Kalinin, and A. A. Vertegel, *Chem. Mater.* **10,** 3548 (1998).
29. R. A. Young, A. Sakthivel, T. S. Moss, and C. O. Paiva-Santos, *J. Appl. Crystallogr.* **28,** 366 (1995).
30. J. Rodríguez-Carbajal, Laboratoire Leon Brillouin (CEA-CNRS), France. Fax: (33) 1 6908 8261. E-mail: juan@llb.saclay.cea.fr.
31. P. Thompson, D. E. Cox, and J. B. Hasting, *J. Appl. Crystallogr.* **20,** 79 (1987).
32. R. A. Young and P. Desai, *Arch. Nauki Mat.* **10,** 71 (1989).
33. E. Prince, *J. Appl. Crystallogr.* **14,** 157 (1981).
34. T. Onui, T. Miyake, K. Fukuda, and Y. Takegami, *Appl. Catal.* **6,** 165 (1983).
35. H. Knözinger and P. Ratnasamy, *Catal. Rev.-Sci. Eng.* **17**, 31 (1978).
36. X. Liu and R. E. Truitt, *J. Am. Chem. Soc.* **119,** 9856 (1997).
37. E. J. Soled, *J. Catal.* **81,** 252 (1983).
38. X. Bokhimi, D. Acosta, J. A. Toledo-Antonio, M. L. Guzmán-Castillo, and F. Hernández-Beltrán, in preparation.
39. Y. Huang, A. White, A. Walpole, and D. L. Trimm, *Appl. Catal.* **56,** 177 (1989).
40. D. Chamma, Doctoral Thesis, Université de Perpignan, France, 1999.